CrossMark

A Novel Method for Achieving Gradient Microstructure in a Cu–Al Alloy: Surface Spinning Strengthening (3S)

Chuan-Xi Ren[1,2] · Qiang Wang[1] · Zhen-Jun Zhang[1] · Yan-Kun Zhu[1] · Zhe-Feng Zhang[1,2]

Abstract A new designed surface strengthening method, surface spinning strengthening (3S), was applied to achieve gradient microstructure in the surface layer of a Cu–11 at.%Al alloy. According to the level of grain refinement, the gradient microstructure can be divided into four zones, including nanoscale grain zone, ultra-fine grain zone, fine grain zone and coarse grain zone from the surface to the matrix. Meanwhile, a plenty of grain boundaries and twin boundaries were introduced to inhibit the dislocation motion in the surface layer during the plastic deformation process. Consequently, the hardened layer with a microhardness gradient and high residual compressive stress was produced on the samples, and the yield strength of the Cu–11 at.%Al alloy was effectively improved after 3S processing due to the strengthening effect caused by the gradient microstructure.

KEY WORDS: Cu–Al alloy; Surface spinning strengthening (3S); Strength; Microhardness; Gradient microstructure

1 Introduction

Fatigue fracture is the most common failure mode for the metallic components bearing the cyclic loading [1]. As is well known that the fatigue crack commonly nucleates at the surface of the metallic components [2], the hardened layer on the metals produced by surface strengthening can effectively restrict the initiation of the fatigue crack, which attracts wide attention in the past years [3, 4]. As the

✉ Qiang Wang
  gmwang@imr.ac.cn

✉ Zhe-Feng Zhang
  zhfzhang@imr.ac.cn

1   Shenyang National Laboratory for Materials Science, Institute of Metal Research, Chinese Academy of Sciences, Shenyang 110016, China

2   School of Materials Science and Engineering, University of Science and Technology of China, Hefei 230026, China

methods of surface strengthening, mechanical surface strengthening processes are widely used to restrict the initiation of fatigue cracks. The strengthening effect derived from the mechanical surface strengthening processes can be mainly attributed to two aspects: the evolution of the microstructure and the introduction of the high residual compressive stress [5, 6]. However, only a few of those methods can cause both microstructural evolution and residual compressive stress in the surface layer of the metallic components.

The evolution of the microstructure in the surface layer of the metallic components, including grain refinement, deformation twinning and dislocation evolution, can effectively improve the surface strength by inhibiting the dislocation movement. For example, surface grinding and surface mechanical grinding treatment (SMGT) are representative methods which can reconstruct the microstructure in the surface layer of metals [7]. Usually, the reconstruction of the microstructure can cause the improvement in the mechanical properties in the surface layer. In this case, the strengthening effect may mainly attribute to the

C.-X. Ren *et al.*: Acta Metall. Sin. (Engl. Lett.), 2017, **30**(3), 212–217

213

introduction of the gradient microstructure in the surface layer. In particular, the nanoscale grains at the topmost surface layer and micrometer-sized coarse grains in the matrix with a transition region between them can be obtained after the treatment. The previous studies have demonstrated that the materials with the gradient nanostructure can effectively extend the fatigue life of metallic materials [5, 8]. Therefore, the evolution of microstructure induced by surface mechanical processing is an effective approach to improve some mechanical properties of the metallic components.

The residual compressive stress can decrease the stress at local area when the component suffers an applied stress and can also restrict the initiation of fatigue cracks [9, 10]. Now according to the theory of surface plastic deformation, the residual compressive stress can be introduced into the surface layer [6]. Among the strengthening methods, shot peening (SP) is a widely accepted surface strengthening method which was developed at the beginning of the last century [9, 11]. Many literatures reported that the residual compressive stress introduced by SP can significantly increase the fatigue life of the metallic components [12]. Some other methods, such as surface rolling strengthening (SRT) [4, 13], surface mechanical attrition treatment (SMAT) [14] and surface mechanical rolling treatment (SMRT) [15], can also create residual compressive stress in the surface layer of the components. Overall, the residual compressive stress may be accepted as a method that can effectively decrease the stress level in the surface layer of the component when it suffers an applied stress in service.

In recent years, some important methods have been developed to prepare high-performance materials by severe plastic deformation (SPD) [16, 17]. However, the surface strengthening methods based on the SPD caused by shear stress need to get more attention and research. In this study, a new method, surface spinning strengthening (3S) (see Fig. 1a), was designed for the purpose of obtaining gradient microstructure in the surface layer due to the surface severe plastic deformation on the plane-type metallic components and the introduction of the residual compressive stress at the same time. The characteristics of 3S are summarized as follows.

1. During the 3S processing, a special machining tool controlled by a milling machine is perpendicular to the metallic component and moves along the processing direction, and the rapid rotation of the machining tool can generate an extremely high shear stress and compressive stress.
2. The shear stress forces the flow of the surface metal layer resulting in the evolution of the microstructure, introducing the residual compressive stress in the surface layer of the metal to some extent.
3. The 3S is a novel method strengthening the surface for metallic materials, especially for plane-type metallic components. By reconstructing the surface microstructure, the components will have some improved properties, like wear resistance and fatigue life. In this study, we will investigate the strengthening effect of the 3S method and provide a better understanding on the surface strengthening mechanism of the metallic component.

2 Experimental

Cu–11 at.%Al alloy (abbreviated as Cu–11Al alloy) was chosen as the target material in this study, and the alloy rod was processed into the billets by wire electrical discharge
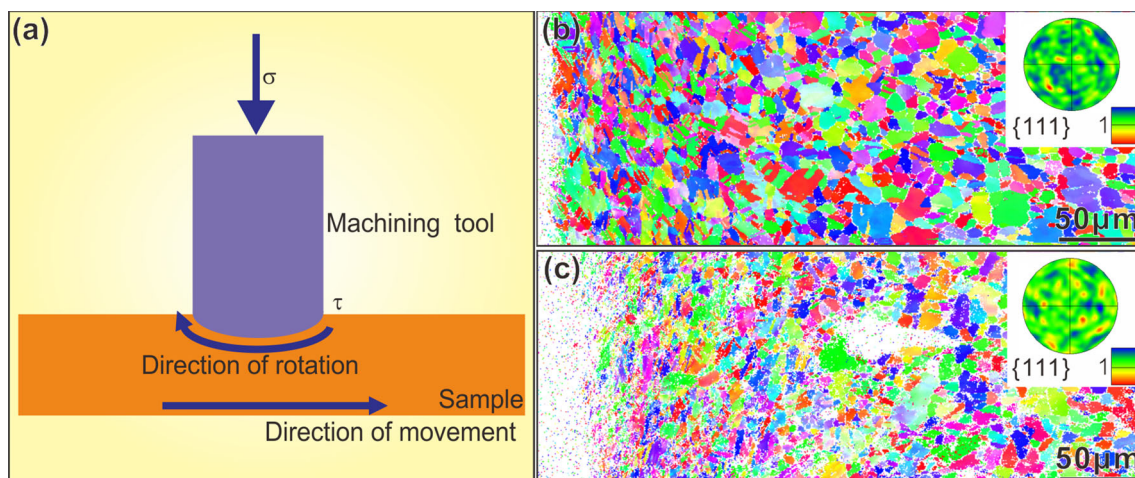

Fig. 1 **a** Schematic illustration of the surface spinning strengthening (3S) setup. 3S-induced gradient microstructures in the surface layer of Cu–11Al-200 sample **b** and Cu–11Al-400 sample **c**, including the orientation distribution maps and the pole figures

machining (WEDM) with a surface area of 16 mm × 16 mm for the following 3S processing. The sample surface was ground to 1500# SiC abrasive paper, cleaned with anhydrous ethanol and dried in cold blowing air. Then, the samples were processed with various feed amounts (defined as the displacement of the machining tool moving in the direction perpendicular to the surface of the sample) at the same machining rate, and meanwhile, the sample surface was cooled by a liquid coolant. The samples processed with the feed amounts of 200 and 400 μm were named as Cu–11Al-200 and Cu–11Al-400, and Cu–11Al-0 without the 3S processing, respectively. Tensile tests were carried out on an Instron 5982 testing machine with a strain rate of 1×10^{-3} s^{-1}. Moreover, the microhardness was tested by an AMH43 full automatic microhardness tester fitted with a Vickers indenter, with a load of 100 g and a holding time of 13 s. The residual stress was measured by Proto LXRD X-ray stress analyzer. The samples for transmission electron microscopy (TEM) were ground to a thickness of ∼0.05 mm and then twin-jet-electropolished at 4–8 °C using a solution of H_3PO_4:C_2H_5OH:H_2O = 1:1:2 (vol.). The samples for electron backscattering diffraction (EBSD) were polished using 2000# SiC abrasive paper and then electrolytic polished at room temperature for ∼60 s using the same solution as the TEM samples. The gradient microstructure of Cu–11Al alloy was characterized by FEI Tecnai F20 (TEM) and LEO SUPRA 35 field emission scanning electron microscopy (SEM).

3 Results and Discussion

After the 3S processing, the orientation image maps and pole figures in the surface layers of the Cu–11Al-200 and Cu–11Al-400 samples are shown in Fig. 1b, c, respectively. The orientation image maps show that the orientation of the grains in the surface layer distributed randomly, and the samples have little deformation texture based on the pole figures. It is clear that the microstructure in the topmost several hundreds of micrometers from the surface to the matrix along the normal direction exhibits a gradient characteristic. As for the SMAT method, the gradient microstructure in the surface layer is constituted of nanostructured layer, fined-grained layer, deformed coarse-grained layer and strain-free coarse-grained matrix layer, owing to the distribution of the gradient strain along the depth [18, 19]. Compared to this division of the gradient microstructure based on grain size and deformation process, we chose an easier approach to understand the change of the grains in the hardened layer.

Based on the observations, the microstructure in the surface layer in the 3S processing can be divided into four zones according to the dimensions of the grains of the two

samples. Taking Cu–11Al-400 as a sample, there is about 50-μm-thick zone where the sizes of most grains are below 100 nm. It means that the deformation in this zone is very severe, which is named as nanoscale grain (NSG) zone. For the pure Cu processed by SMAT, a nanostructured surface layer of about 35 μm thick was formed [18]. The zone from ∼50 to ∼100 μm is named as ultra-fine grain (UFG) zone where the grains are refined from several hundreds of nanometers to one micrometer. In the next zone between the matrix and the UFG zone, the grains are refined to several micrometers, which is named as fine grain (FG) zone. The last zone is coarse grain (CG) zone in the matrix. The above four zones constitute the gradient microstructure of the Cu–11Al alloy processed by 3S method.

Figure 2 presents the typical bright-field TEM micrographs of the FG zone for Cu–11Al-200 (Fig. 2a) and Cu–11Al-400 (Fig. 2b) samples after 3S processing. It is well known that slip and twinning are two plastic deformation modes in the face-centered cubic (fcc) metals and alloys [20, 21]. Commonly, the Cu–11Al alloy has lower stacking fault energy (SFE) than the pure Cu, and twinning is one of the major deformation modes, so it is easier to introduce deformation twins during the 3S processing [22–24]. Abundant deformation twins appear, and twin bands intersect with each other in the FG zone in the surface layer of the Cu–11Al alloy after the 3S processing. As shown in Fig. 2c, d, the grains are refined to a dimension of dozens of nanometers, about 50–100 nm or even less. Hence, the 3S processing is a novel method for surface nanocrystallization.

As shown in Fig. 3a, the average microhardness of the Cu–11Al-0 sample is ∼136.1 HV. After the 3S processing, the microhardness in the surface layer of the Cu–11Al-200 sample is enhanced significantly, and the maximum value of the microhardness is about 238.2 HV, that is to say, the microhardness increases by about 75.0% in the topmost surface layer. Similarly, the maximum value of the microhardness in the topmost surface layer of Cu–11Al-400 sample is about 247.6 HV, which is a little bit higher than that of Cu–11Al-200 sample. The microhardness curves of Cu–11Al-200 and Cu–11Al-400 samples change gradually, and they can be expressed an equation with the depth, d, as follows:

$$Hv = Hv^{m} + \Delta Hv \cdot e^{Rd}, \qquad (1)$$

where Hv is the microhardness at some point in the surface layer of the sample, Hv^{m} is the value of the microhardness in the matrix, d is the distance of the point to the surface, R is the hardening exponent, and ΔHv is the maximum increment in the microhardness, as follows:

$$\Delta Hv = Hv^{M} - Hv^{m}, \qquad (2)$$

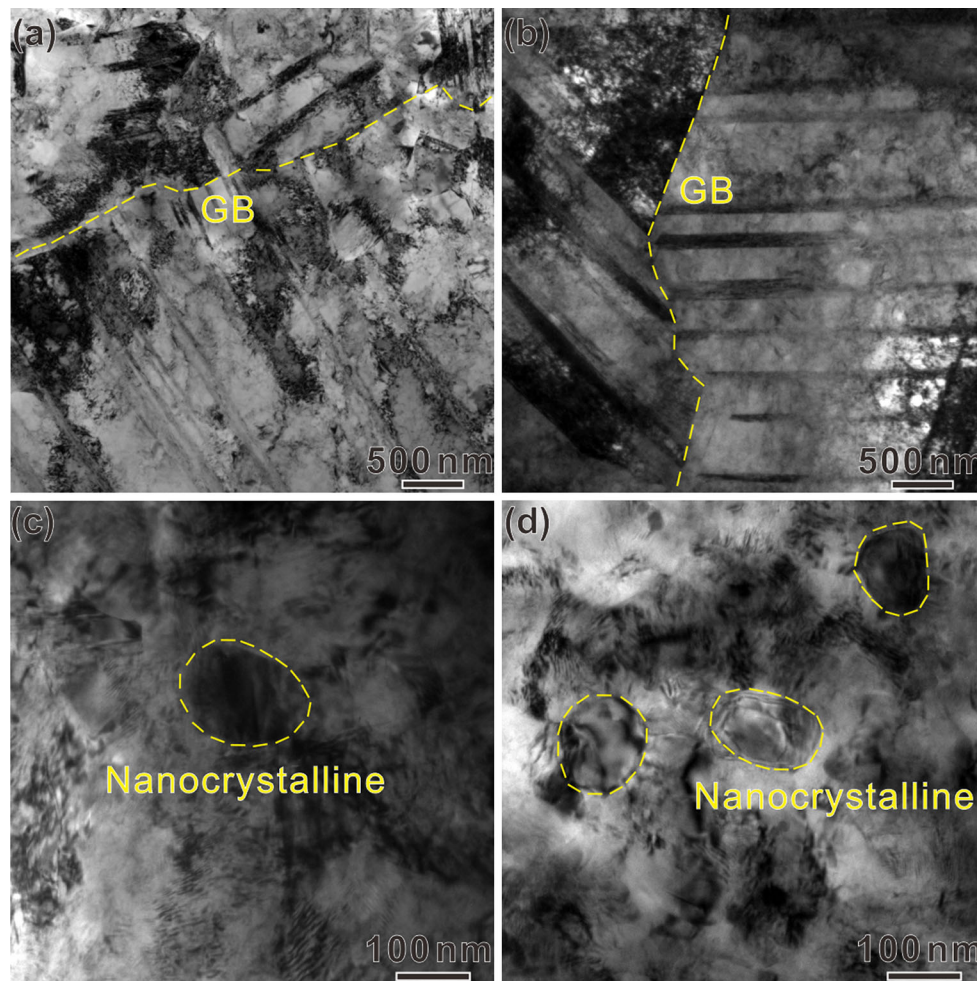where Hv^{M} is the maximum value of the microhardness in the surface layer.

Fig. 2 TEM micrographs of Cu–11Al alloy: **a** Cu–11Al-200 sample in the fine grain zone, **b** Cu–11Al-400 sample in the fine grain zone, **c** Cu–11Al-200 sample in the nanoscale grain zone, **d** Cu–11Al-400 sample in the nanoscale grain zone
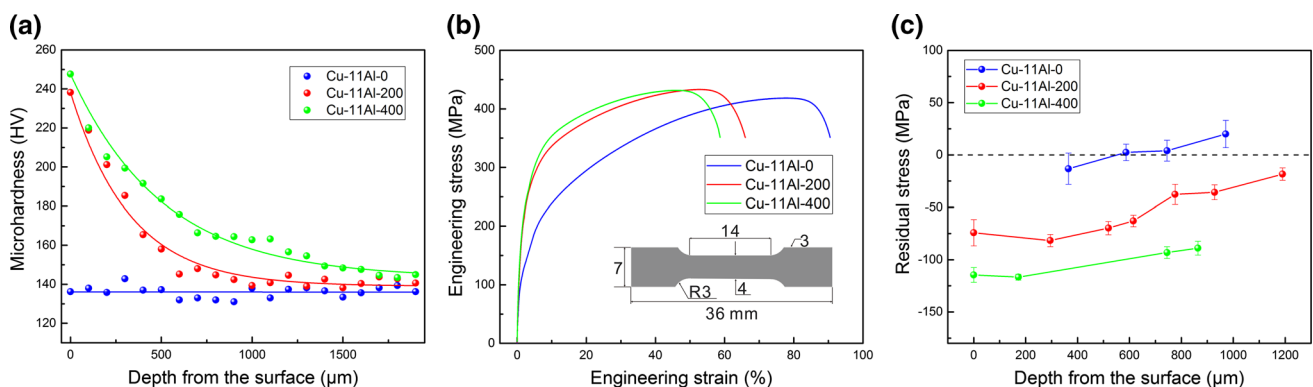

Fig. 3 **a** Variation of the gradient mechanical property of Cu–11Al alloy with the depth from the surface, **b** tensile engineering stress–strain curves of Cu–11Al alloy with different 3S processing feed amounts, **c** residual stress profiles following different 3S processing depths on Cu–11Al alloy

In the 3S processing, Hv^{M} is the maximum microhardness achieved by the 3S processing and also strongly depends on the nature of materials. ΔHv is related to the 3S feed amount. By controlling the different 3S feed amounts,
different ΔHv of hardened layer can be achieved. For Cu–11Al alloy, ΔHv is 102.1 HV, and R is -0.0028 in Cu–11Al-200 sample, while ΔHv is 111.5 HV, and R is -0.0016 in Cu–11Al-400 sample. Generally, the hardened

layer can be defined as the zone in which the microhardness is significantly different from the matrix [25]. When the microhardness in the hardened layer decreases to Hv^m +10 (HV), there is little effect on the strengthening, and the thickness of the hardened layer is defined by this depth from the surface when the microhardness value is Hv^m +10 (HV). For the Cu–11Al-200 sample, the 3S processing can create a hardened layer with the thickness of about 830 μm; however, for the Cu–11Al-400 sample, the thickness of the hardened layer achieves about 1507 μm, which is significantly thicker than that of the Cu–11Al-200 sample.

The thickness of the hardened layer is also different depending on the processing method and the categories of materials. For example, the AISI 316L stainless steel processed by SMRT has a depth of ∼1 mm with a gradient nanostructured surface layer [5]. For ultrasonic surface rolling process (USPP), the hardness at the top surface increases from the initial state to 385 HV, and the hardened layer thickness is about 300 μm in Ti–6Al–4V [10]. Additionally, the decreasing rate of the microhardness in the surface layer of Cu–11Al-400 sample is obviously slower than that of Cu–11Al-200 sample. Therefore, the value of R represents the decreasing tendency of the microhardness from the surface to matrix in the hardened layer. R of Cu–11Al-400 sample is larger, and this result indicates that the strengthening effect may be improved with the increase in the feed amount of 3S processing.

In addition to the hardness, the yield strength of Cu–11Al alloy can also be improved by surface strengthening on the basis of the tensile stress–strain curves as shown in Fig. 3b. For the Cu–11Al-200 sample, the yield strength increases from ∼80 MPa (Cu–11Al-0) to ∼140 MPa, while for the Cu–11Al-400 sample, the yield strength increases to ∼160 MPa. Commonly, the strength and ductility are mutually exclusive in metallic materials, and elongation to failure is a measure of the material ductility [17, 26]. With increasing 3S feed amount, the elongation of Cu–11Al-200 sample decreases from ∼80 to ∼55% and the elongation of Cu–11Al-400 sample decreases to ∼45%. For ultimate tensile strength, it is about 420 MPa (Cu–11Al-0), 433 MPa (Cu–11Al-200) and 431 MPa (Cu–11Al-400), respectively. It seems that the 3S processing only influences a little on the ultimate tensile strength of Cu–11Al alloy. The major reason for the improvement in yield strength is that the surface microstructure in the hardened layer was modified by the 3S processing. The Cu–11Al-400 sample has a higher increase in the yield strength due to the thicker hardened layer. Different from Cu–Al alloys, the texture in the hardened layer is also important to the yield strength for some other materials [27]. In the 3S processing, the improvement in yield strength can be regarded as the grain refinement

strengthening and strain strengthening in the surface-hardened layer, and this is a result of hindering the dislocation motion [28].

Besides the microstructure evolution, the residual stress is also widely accepted as a parameter to evaluate the effect of the surface strengthening [29, 30]. The residual stress of Cu–11Al alloy with the 3S treatment was also measured, and the results are shown in Fig. 3c. With increasing 3S feed amount from 200 to 400 μm, the maximum residual compressive stress increases from −74.20 (Cu–11Al-200) to −114.56 MPa (Cu–11Al-400). From NSG to CG zone, the residual compressive stress decreases constantly in Cu–11Al-200 and Cu–11Al-400 samples. The residual stress is commonly caused by the plastic incompatibility stress, intergranular stress, and so on during the plastic deformation [6, 8, 29]. Undoubtedly, Cu–11Al-400 sample obtains the highest residual compressive stress in the surface layer, and Cu–11Al-400 sample experienced severer plastic deformation during the 3S process.

Furthermore, the relation between the microhardness and the gradient microstructure in the hardened layer is schematically shown in Fig. 4. In the NSG zone, the grains are refined to nanoscale grains induced by the very severe plastic deformation. The grains in the UFG zone are also refined, but the level of the refinement is in between the NSG zone and the FG zone. In addition, abundant twins were induced into the refined grains. It was reported that those GBs and TBs can impede the movement of dislocations in the UFG zone [31, 32]. With the cooperation of TBs and GBs, the dislocation motion is also limited in the FG zone. Meanwhile, there are plenty of dislocations, GBs and deformation twins, increasing the flow stress of
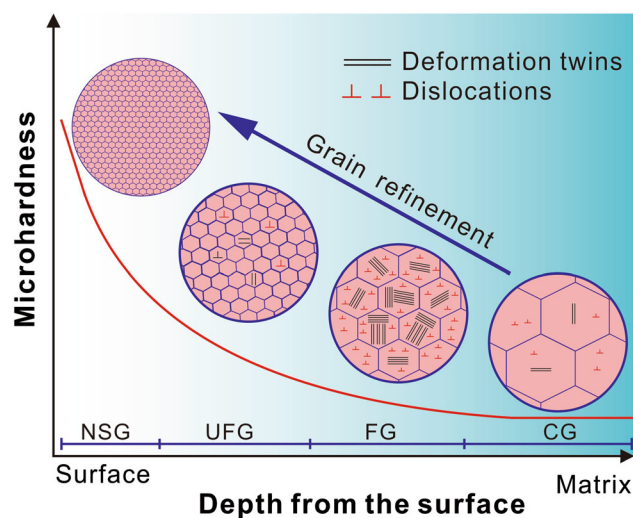

Fig. 4 Schematic illustration of the variation of the microhardness with the depth from the surface, and the gradient microstructure with grain refinement in the surface layer of Cu–11Al alloy processed by the 3S method

dislocations [33, 34]. Therefore, the surface layer of the Cu–11Al alloy was strengthened during the 3S processing. From the CG zone to the NSG zone, the plastic deformation is weakened gradually along the normal direction, and the grains of Cu–11Al alloy are also refined gradually. For the microhardness in the hardened layer, the microhardness decreases gradually with increasing depth to the surface in an exponent type, and the microstructure also changes accordingly. The evolution of the microstructure results in the increase in the microhardness in the surface layer of Cu–11Al alloy, and a hardened layer is created on Cu–11Al alloy. In the hardened layer, the two major strengthening mechanisms are grain refinement strengthening and strain strengthening [35–37], and the grain refinement plays a dominant role in the strengthening of the NSG and UFG zone.

4 Conclusion

It is confirmed that 3S is an effective method to enhance the yield strength and surface hardness, extend the hardened layer thickness, introduce the residual stress and obtain the gradient microstructure. The microstructure in the surface layer of Cu–11Al alloy changes gradually and exhibits a gradient characteristic. Furthermore, the gradient microstructure can be divided into four zones, including NSG zone, UGF zone, FG zone and CG zone, according to the level of the grain refinement. In addition, the yield strength of the Cu–11Al alloy treated by 3S was significantly improved. The high residual compressive stress was introduced into the surface layer of Cu–11Al alloy. The microhardness in the hardened layer decreased gradually with the depth form the surface, and the thickness of the hardened layer increases markedly with increasing 3S feed amount.

References

[1] E.P. Busso, S.D. Antolovich, Acta Mater. **107**, 484 (2016)
[2] R.O. Ritchie, Int. J. Fract. **100**, 55 (1999)
[3] A. Pineau, A. Amine Benzerga, T. Pardoen, Acta Mater. **107**, 508 (2016)
[4] N. Tsuji, S. Tanaka, T. Takasugi, Mater. Sci. Eng. A **488**, 139 (2008)
[5] H.W. Huang, Z.B. Wang, J. Lu, K. Lu, Acta Mater. **87**, 150 (2015)
[6] P.J. Withers, Rep. Prog. Phys. **70**, 2211 (2007)
[7] T.H. Fang, W.L. Li, N.R. Tao, K. Lu, Science **331**, 1587 (2011)
[8] T. Roland, D. Retraint, K. Lu, J. Lu, Scr. Mater. **54**, 1949 (2006)
[9] V. Llaneza, F.J. Belzunce, Appl. Surf. Sci. **356**, 475 (2015)
[10] H.B. Wang, G.L. Song, G.Y. Tang, J. Alloys Compd. **681**, 146 (2016)
[11] N. Tsuji, S. Tanaka, T. Takasugi, Surf. Coat. Technol. **203**, 1400 (2009)
[12] M.A.S. Torres, H.J.C. Voorwald, Int. J. Fatigue **24**, 877 (2002)
[13] C. Yuan, R.D. Fu, F.C. Zhang, X.Y. Zhang, F.C. Liu, Mater. Sci. Eng. A **565**, 27 (2013)
[14] Y.M. Lin, J. Lu, L.P. Wang, T. Xu, Q.J. Xue, Acta Mater. **54**, 5599 (2006)
[15] X.C. Liu, H.W. Zhang, K. Lu, Science **342**, 337 (2013)
[16] K.S. Kumar, H. Van Swygenhoven, S. Suresh, Acta Mater. **51**, 5743 (2003)
[17] R.Z. Valiev, Nat. Mater. **3**, 511 (2004)
[18] K. Lu, J. Lu, Mater. Sci. Eng. A **375**, 38 (2004)
[19] T. Roland, D. Retraint, K. Lu, J. Lu, Mater. Sci. Eng. A **445**, 281 (2007)
[20] J. Hirsch, K. Lucke, M. Hatherly, Acta Metall. **36**, 2905 (1988)
[21] J.W. Christian, S. Mahajan, Prog. Mater. Sci. **39**, 1 (1995)
[22] X.H. An, Q.Y. Lin, S.D. Wu, Z.F. Zhang, R.B. Figueiredo, T.G. Langdon, Philos. Mag. **91**, 3307 (2011)
[23] R. Liu, Z.J. Zhang, Z.F. Zhang, Mater. Sci. Eng. A **666**, 123 (2016)
[24] X.H. An, Q.Y. Lin, S.D. Wu, Z.F. Zhang, R.B. Figueiredo, N. Gao, T.G. Langdon, Scr. Mater. **64**, 954 (2011)
[25] C. Ye, A. Telang, A.S. Gill, S. Suslov, Y. Idell, K. Zweiacker, J.M.K. Wiezorek, Z. Zhou, D. Qian, S.R. Mannava, V.K. Vasudevan, Mater. Sci. Eng. A **613**, 274 (2014)
[26] M.A. Meyers, A. Mishra, D.J. Benson, Prog. Mater Sci. **51**, 427 (2006)
[27] G.Z. Voyiadjis, B. Deliktas, Int. J. Plast. **25**, 1997 (2009)
[28] D. Kiener, A.M. Minor, Acta Mater. **59**, 1328 (2011)
[29] F. Macionczyk, W. Bruckner, J. Appl. Phys. **86**, 4922 (1999)
[30] A.H. Heuer, F. Ernst, H. Kahn, A. Avishai, G.M. Michal, D.J. Pitchure, R.E. Ricker, Scr. Mater. **56**, 1067 (2007)
[31] K. Lu, L. Lu, S. Suresh, Science **324**, 349 (2009)
[32] V. Yamakov, D. Wolf, S.R. Phillpot, A.K. Mukherjee, H. Gleiter, Nat. Mater. **1**, 45 (2002)
[33] J. Wang, X. Zhang, MRS Bull. **41**, 274 (2016)
[34] M.L. Kronberg, Acta Metall. **5**, 507 (1957)
[35] N. Tsuji, Y. Saito, H. Utsunomiya, S. Tanigawa, Scr. Mater. **40**, 795 (1999)
[36] Y.Z. Tian, J.J. Li, P. Zhang, S.D. Wu, Z.F. Zhang, M. Kawasaki, T.G. Langdon, Acta Mater. **60**, 269 (2012)
[37] L. Bardella, A. Panteghini, J. Mech. Phys. Solids **78**, 467 (2015)